

Measurements of time-dependent CP violation in $B^0 \rightarrow \omega K_S^0$, $f_0(980)K_S^0$, $K_S^0\pi^0$ and $K^+K^-K_S^0$ decays

K. Abe,⁹ K. Abe,⁴⁹ I. Adachi,⁹ H. Aihara,⁵¹ D. Anipko,¹ K. Aoki,²⁵ T. Arakawa,³²
K. Arinstein,¹ Y. Asano,⁵⁶ T. Aso,⁵⁵ V. Aulchenko,¹ T. Aushev,²¹ T. Aziz,⁴⁷ S. Bahinipati,⁴
A. M. Bakich,⁴⁶ V. Balagura,¹⁵ Y. Ban,³⁷ S. Banerjee,⁴⁷ E. Barberio,²⁴ M. Barbero,⁸
A. Bay,²¹ I. Bedny,¹ K. Belous,¹⁴ U. Bitenc,¹⁶ I. Bizjak,¹⁶ S. Blyth,²⁷ A. Bondar,¹
A. Bozek,³⁰ M. Bračko,^{23,16} J. Brodzicka,^{9,30} T. E. Browder,⁸ M.-C. Chang,⁵⁰ P. Chang,²⁹
Y. Chao,²⁹ A. Chen,²⁷ K.-F. Chen,²⁹ W. T. Chen,²⁷ B. G. Cheon,³ R. Chistov,¹⁵
J. H. Choi,¹⁸ S.-K. Choi,⁷ Y. Choi,⁴⁵ Y. K. Choi,⁴⁵ A. Chuvikov,³⁹ S. Cole,⁴⁶ J. Dalseno,²⁴
M. Danilov,¹⁵ M. Dash,⁵⁷ R. Dowd,²⁴ J. Dragic,⁹ A. Drutskoy,⁴ S. Eidelman,¹ Y. Enari,²⁵
D. Epifanov,¹ S. Fratina,¹⁶ H. Fujii,⁹ M. Fujikawa,²⁶ N. Gabyshev,¹ A. Garmash,³⁹
T. Gershon,⁹ A. Go,²⁷ G. Gokhroo,⁴⁷ P. Goldenzweig,⁴ B. Golob,^{22,16} A. Gorišek,¹⁶
M. Grossé Perdekamp,^{11,40} H. Guler,⁸ H. Ha,¹⁸ J. Haba,⁹ K. Hara,²⁵ T. Hara,³⁵
Y. Hasegawa,⁴⁴ N. C. Hastings,⁵¹ K. Hayasaka,²⁵ H. Hayashii,²⁶ M. Hazumi,⁹
D. Heffernan,³⁵ T. Higuchi,⁹ L. Hinz,²¹ T. Hokuue,²⁵ Y. Hoshi,⁴⁹ K. Hoshina,⁵⁴ S. Hou,²⁷
W.-S. Hou,²⁹ Y. B. Hsiung,²⁹ Y. Igarashi,⁹ T. Iijima,²⁵ K. Ikado,²⁵ A. Imoto,²⁶ K. Inami,²⁵
A. Ishikawa,⁵¹ H. Ishino,⁵² K. Itoh,⁵¹ R. Itoh,⁹ M. Iwabuchi,⁶ M. Iwasaki,⁵¹ Y. Iwasaki,⁹
C. Jacoby,²¹ M. Jones,⁸ H. Kakuno,⁵¹ J. H. Kang,⁵⁸ J. S. Kang,¹⁸ P. Kapusta,³⁰
S. U. Kataoka,²⁶ N. Katayama,⁹ H. Kawai,² T. Kawasaki,³² H. R. Khan,⁵² A. Kibayashi,⁵²
H. Kichimi,⁹ N. Kikuchi,⁵⁰ H. J. Kim,²⁰ H. O. Kim,⁴⁵ J. H. Kim,⁴⁵ S. K. Kim,⁴³
T. H. Kim,⁵⁸ Y. J. Kim,⁶ K. Kinoshita,⁴ N. Kishimoto,²⁵ S. Korpar,^{23,16} Y. Kozakai,²⁵
P. Križan,^{22,16} P. Krokovny,⁹ T. Kubota,²⁵ R. Kulásík,⁴ R. Kumar,³⁶ C. C. Kuo,²⁷
E. Kurihara,² A. Kusaka,⁵¹ A. Kuzmin,¹ Y.-J. Kwon,⁵⁸ J. S. Lange,⁵ G. Leder,¹³ J. Lee,⁴³
S. E. Lee,⁴³ Y.-J. Lee,²⁹ T. Lesiak,³⁰ J. Li,⁸ A. Limosani,⁹ C. Y. Lin,²⁹ S.-W. Lin,²⁹
Y. Liu,⁶ D. Liventsev,¹⁵ J. MacNaughton,¹³ G. Majumder,⁴⁷ F. Mandl,¹³ D. Marlow,³⁹
T. Matsumoto,⁵³ A. Matyja,³⁰ S. McOnie,⁴⁶ T. Medvedeva,¹⁵ Y. Mikami,⁵⁰ W. Mitaroff,¹³
K. Miyabayashi,²⁶ H. Miyake,³⁵ H. Miyata,³² Y. Miyazaki,²⁵ R. Mizuk,¹⁵ D. Mohapatra,⁵⁷
G. R. Moloney,²⁴ T. Mori,⁵² J. Mueller,³⁸ A. Murakami,⁴¹ T. Nagamine,⁵⁰ Y. Nagasaka,¹⁰
T. Nakagawa,⁵³ Y. Nakahama,⁵¹ I. Nakamura,⁹ E. Nakano,³⁴ M. Nakao,⁹ H. Nakazawa,⁹
Z. Natkaniec,³⁰ K. Neichi,⁴⁹ S. Nishida,⁹ K. Nishimura,⁸ O. Nitoh,⁵⁴ S. Noguchi,²⁶
T. Nozaki,⁹ A. Ogawa,⁴⁰ S. Ogawa,⁴⁸ T. Ohshima,²⁵ T. Okabe,²⁵ S. Okuno,¹⁷ S. L. Olsen,⁸
S. Ono,⁵² W. Ostrowicz,³⁰ H. Ozaki,⁹ P. Pakhlov,¹⁵ G. Pakhlova,¹⁵ H. Palka,³⁰
C. W. Park,⁴⁵ H. Park,²⁰ K. S. Park,⁴⁵ N. Parslow,⁴⁶ L. S. Peak,⁴⁶ M. Pernicka,¹³
R. Pestotnik,¹⁶ M. Peters,⁸ L. E. Piilonen,⁵⁷ A. Poluektov,¹ F. J. Ronga,⁹ N. Root,¹
J. Rorie,⁸ M. Rozanska,³⁰ H. Sahoo,⁸ S. Saitoh,⁹ Y. Sakai,⁹ H. Sakamoto,¹⁹ H. Sakaue,³⁴
T. R. Sarangi,⁶ N. Sato,²⁵ N. Satoyama,⁴⁴ K. Sayeed,⁴ T. Schietinger,²¹ O. Schneider,²¹
P. Schönmeier,⁵⁰ J. Schümänn,²⁸ C. Schwanda,¹³ A. J. Schwartz,⁴ R. Seidl,^{11,40} T. Seki,⁵³
K. Senyo,²⁵ M. E. Sevior,²⁴ M. Shapkin,¹⁴ Y.-T. Shen,²⁹ H. Shibuya,⁴⁸ B. Shwartz,¹
V. Sidorov,¹ J. B. Singh,³⁶ A. Sokolov,¹⁴ A. Somov,⁴ N. Soni,³⁶ R. Stamen,⁹ S. Stanic,³³
M. Staric,¹⁶ H. Stoeck,⁴⁶ A. Sugiyama,⁴¹ K. Sumisawa,⁹ T. Sumiyoshi,⁵³ S. Suzuki,⁴¹
S. Y. Suzuki,⁹ O. Tajima,⁹ N. Takada,⁴⁴ F. Takasaki,⁹ K. Tamai,⁹ N. Tamura,³²

K. Tanabe,⁵¹ M. Tanaka,⁹ G. N. Taylor,²⁴ Y. Teramoto,³⁴ X. C. Tian,³⁷ I. Tikhomirov,¹⁵
K. Trabelsi,⁹ Y. T. Tsai,²⁹ Y. F. Tse,²⁴ T. Tsuboyama,⁹ T. Tsukamoto,⁹ K. Uchida,⁸
Y. Uchida,⁶ S. Uehara,⁹ T. Uglov,¹⁵ K. Ueno,²⁹ Y. Unno,⁹ S. Uno,⁹ P. Urquijo,²⁴
Y. Ushiroda,⁹ Y. Usov,¹ G. Varner,⁸ K. E. Varvell,⁴⁶ S. Villa,²¹ C. C. Wang,²⁹
C. H. Wang,²⁸ M.-Z. Wang,²⁹ M. Watanabe,³² Y. Watanabe,⁵² J. Wicht,²¹ L. Widhalm,¹³
J. Wiechczynski,³⁰ E. Won,¹⁸ C.-H. Wu,²⁹ Q. L. Xie,¹² B. D. Yabsley,⁴⁶ A. Yamaguchi,⁵⁰
H. Yamamoto,⁵⁰ S. Yamamoto,⁵³ Y. Yamashita,³¹ M. Yamauchi,⁹ Heyoung Yang,⁴³
S. Yoshino,²⁵ Y. Yuan,¹² Y. Yusa,⁵⁷ S. L. Zang,¹² C. C. Zhang,¹² J. Zhang,⁹
L. M. Zhang,⁴² Z. P. Zhang,⁴² V. Zhilich,¹ T. Ziegler,³⁹ A. Zupanc,¹⁶ and D. Zürcher²¹

(The Belle Collaboration)

¹Budker Institute of Nuclear Physics, Novosibirsk

²Chiba University, Chiba

³Chonnam National University, Kwangju

⁴University of Cincinnati, Cincinnati, Ohio 45221

⁵University of Frankfurt, Frankfurt

⁶The Graduate University for Advanced Studies, Hayama

⁷Gyeongsang National University, Chinju

⁸University of Hawaii, Honolulu, Hawaii 96822

⁹High Energy Accelerator Research Organization (KEK), Tsukuba

¹⁰Hiroshima Institute of Technology, Hiroshima

¹¹University of Illinois at Urbana-Champaign, Urbana, Illinois 61801

¹²Institute of High Energy Physics,

Chinese Academy of Sciences, Beijing

¹³Institute of High Energy Physics, Vienna

¹⁴Institute of High Energy Physics, Protvino

¹⁵Institute for Theoretical and Experimental Physics, Moscow

¹⁶J. Stefan Institute, Ljubljana

¹⁷Kanagawa University, Yokohama

¹⁸Korea University, Seoul

¹⁹Kyoto University, Kyoto

²⁰Kyungpook National University, Taegu

²¹Swiss Federal Institute of Technology of Lausanne, EPFL, Lausanne

²²University of Ljubljana, Ljubljana

²³University of Maribor, Maribor

²⁴University of Melbourne, Victoria

²⁵Nagoya University, Nagoya

²⁶Nara Women's University, Nara

²⁷National Central University, Chung-li

²⁸National United University, Miao Li

²⁹Department of Physics, National Taiwan University, Taipei

³⁰H. Niewodniczanski Institute of Nuclear Physics, Krakow

³¹Nippon Dental University, Niigata

³²Niigata University, Niigata

³³University of Nova Gorica, Nova Gorica

³⁴Osaka City University, Osaka

³⁵Osaka University, Osaka

³⁶*Panjab University, Chandigarh*

³⁷*Peking University, Beijing*

³⁸*University of Pittsburgh, Pittsburgh, Pennsylvania 15260*

³⁹*Princeton University, Princeton, New Jersey 08544*

⁴⁰*RIKEN BNL Research Center, Upton, New York 11973*

⁴¹*Saga University, Saga*

⁴²*University of Science and Technology of China, Hefei*

⁴³*Seoul National University, Seoul*

⁴⁴*Shinshu University, Nagano*

⁴⁵*Sungkyunkwan University, Suwon*

⁴⁶*University of Sydney, Sydney NSW*

⁴⁷*Tata Institute of Fundamental Research, Bombay*

⁴⁸*Toho University, Funabashi*

⁴⁹*Tohoku Gakuin University, Tagajo*

⁵⁰*Tohoku University, Sendai*

⁵¹*Department of Physics, University of Tokyo, Tokyo*

⁵²*Tokyo Institute of Technology, Tokyo*

⁵³*Tokyo Metropolitan University, Tokyo*

⁵⁴*Tokyo University of Agriculture and Technology, Tokyo*

⁵⁵*Toyama National College of Maritime Technology, Toyama*

⁵⁶*University of Tsukuba, Tsukuba*

⁵⁷*Virginia Polytechnic Institute and State University, Blacksburg, Virginia 24061*

⁵⁸*Yonsei University, Seoul*

Abstract

We present measurements of time-dependent CP asymmetries in $B^0 \rightarrow \omega K_S^0$, $f_0(980)K_S^0$, $K_S^0\pi^0$ and $K^+K^-K_S^0$ based on a sample of 535×10^6 $B\bar{B}$ pairs collected at the $\Upsilon(4S)$ resonance with the Belle detector at the KEKB energy-asymmetric e^+e^- collider. One neutral B meson is fully reconstructed in one of the specified decay channels, and the flavor of the accompanying B meson is identified from its decay products. CP -violation parameters for each of the decay modes are obtained from the asymmetries in the distributions of the proper-time intervals between the two B decays.

PACS numbers: 11.30.Er, 12.15.Hh, 13.25.Hw

The Standard Model (SM) describes CP violation in B^0 meson decays using the complex phase of the 3×3 Cabibbo-Kobayashi-Maskawa (CKM) mixing matrix [1]. CP asymmetries in neutral B meson decays into CP eigenstates f exhibit a time-dependent behavior

$$A(\Delta t) = \mathcal{S}_f \sin(\Delta m_d \Delta t) + \mathcal{A}_f \cos(\Delta m_d \Delta t) \quad (1)$$

where \mathcal{S}_f and \mathcal{A}_f are the CP violation parameters, Δm_d the mass difference between the two B^0 mass eigenstates, Δt the difference between the decay time of the signal B^0 (\overline{B}^0) and of the opposite-side \overline{B}^0 (B^0). The SM predicts that for most of the decays that proceed via the quark transitions $b \rightarrow s\bar{q}q$ ($q = u, d, s$) the relations $\mathcal{S}_f = -\xi_f \sin 2\phi_1$ and $\mathcal{A}_f \simeq 0$, where $\xi_f = +1(-1)$ corresponds to CP -even (-odd) final states, hold to a good approximation [2]. With physics beyond the SM, these decays may receive significant contributions that depend on a phase that is different from the SM prediction. A comparison of the effective $\sin 2\phi_1$ values, $\sin 2\phi_1^{eff}$, with $\sin 2\phi_1$ obtained from the decays governed by the $b \rightarrow c\bar{c}s$ transition is thus an important test of the SM.

Among the final states studied, ωK_S^0 and $K_S^0\pi^0$ are CP -odd modes, $f_0(980)K_S^0$ is a CP -even mode, while $K^+K^-K_S^0$ is a mixture of both $\xi_f = -1$ and $+1$. The SM expectation for this latter mode is $\mathcal{S}_f = -(2f_+ - 1)\sin 2\phi_1$, where f_+ is the CP -even fraction. A measurement of f_+ was obtained using isospin relation [6] with a 357 fb^{-1} data sample and gives $f_+ = 0.93 \pm 0.09(\text{stat}) \pm 0.05(\text{syst})$.

Recently, it was found that the direct CP asymmetries in $B^0 \rightarrow K^+\pi^-$ and $B^+ \rightarrow K^+\pi^0$ differ significantly [3] while they were naively expected to be same [4]. Using the $B^0 \rightarrow K_S\pi^0$ result, an additional test to understand the situation can be made by comparing the measured \mathcal{A}_f value and the value predicted by a sum rule [5] using asymmetry measurements from the other $B \rightarrow K\pi$ decays.

Previous measurements of CP asymmetries in $b \rightarrow s\bar{q}q$ transitions have been reported by Belle [7] and BaBar [8]. Belle's previously published results of CP in $B^0 \rightarrow \omega K_S^0$, $f_0(980)K_S^0$, $K_S^0\pi^0$ and $K^+K^-K_S^0$ were based on a 253 fb^{-1} data sample corresponding to $275 \times 10^6 B\overline{B}$ pairs. In this report, we describe improved measurements incorporating an additional 239 fb^{-1} data sample for a total of 492 fb^{-1} ($535 \times 10^6 B\overline{B}$ pairs).

At the KEKB energy-asymmetric e^+e^- (3.5 on 8.0 GeV) collider, the $\Upsilon(4S)$ is produced with a Lorentz boost of $\beta\gamma = 0.425$ nearly along the electron beamline (z). Since the B^0 and \overline{B}^0 are approximatively at rest in the $\Upsilon(4S)$ center-of-mass system (cms), Δt can be determined from the displacement in z between the two decay vertices: $\Delta t \equiv \Delta z / (\beta\gamma c)$.

The Belle detector is a large-solid-angle magnetic spectrometer that consists of a silicon vertex detector (SVD), a 50-layer central drift chamber (CDC), an array of aerogel threshold Čerenkov counters (ACC), a barrel-like arrangement of time-of-flight scintillation counters (TOF), and an electromagnetic calorimeter (ECL) comprised of CsI(Tl) crystals located inside a superconducting solenoid coil that provides a 1.5 T magnetic field. An iron flux-return located outside of the coil is instrumented to detect K_L^0 mesons and to identify muons (KLM). The detector is described in detail elsewhere [10]. Two different inner detector configurations were used. For the first sample of $152 \times 10^6 B\overline{B}$ pairs, a 2.0 cm radius beampipe and a 3-layer silicon vertex detector were used; for the latter $383 \times 10^6 B\overline{B}$ pairs, a 1.5 cm radius beampipe, a 4-layer silicon detector and a small-cell inner drift chamber were used [11].

We reconstruct the following B^0 decay modes to measure CP asymmetries: $B^0 \rightarrow \omega K_S^0$, $f_0(980)K_S^0$, $K_S^0\pi^0$ and $K^+K^-K_S^0$. We exclude K^+K^- pairs that are consistent with a $\phi \rightarrow K^+K^-$ decay from the $K^+K^-K_S^0$ sample. The intermediate meson states are reconstructed

from the following decays: $\pi^0 \rightarrow \gamma\gamma$, $K_S^0 \rightarrow \pi^+\pi^-$, $\omega \rightarrow \pi^+\pi^-\pi^0$ and $f_0(980) \rightarrow \pi^+\pi^-$. Charged tracks reconstructed with the CDC, except for tracks from $K_S^0 \rightarrow \pi^+\pi^-$ decays, are required to originate from the interaction point (IP). We distinguish charged kaons from pions based on a kaon (pion) likelihood $\mathcal{L}_{K(\pi)}$ derived from the TOF, ACC and dE/dx measurements in the CDC. Photons are identified as isolated ECL clusters that are not matched to any charged track.

We identify B meson decays using the energy difference $\Delta E \equiv E_B^{\text{cms}} - E_{\text{beam}}^{\text{cms}}$ and the beam-energy constrained mass $M_{\text{bc}} \equiv \sqrt{(E_{\text{beam}}^{\text{cms}})^2 - (p_B^{\text{cms}})^2}$, where $E_{\text{beam}}^{\text{cms}}$ is the beam energy in the cms, and E_B^{cms} and p_B^{cms} are the cms energy and momentum of the reconstructed B candidate, respectively. The signal candidates are selected by requiring $5.27 \text{ GeV}/c^2 < M_{\text{bc}} < 5.29 \text{ GeV}/c^2$ and a mode-dependent ΔE window. The dominant background for the $b \rightarrow s\bar{q}q$ signal comes from continuum events ($e^+e^- \rightarrow u\bar{u}, d\bar{d}, s\bar{s}, c\bar{c}$). We discriminate against this using event topology: continuum events tend to be jet-like in the cms, while $e^+e^- \rightarrow B\bar{B}$ events tend to be spherical. To quantify event topology, we calculate modified Fox-Wolfram moments and combine them into a Fisher discriminant [12]. We calculate a probability density function (PDF) for this discriminant and multiply it by a PDF for $\cos\theta_B$, where θ_B is the polar angle in the cms between the B direction and the beam axis. The PDFs for signal and continuum are obtained from Monte Carlo (MC) simulation and a data sideband, respectively. These PDFs are then used to calculate a signal [background] likelihood $\mathcal{L}_{\text{sig[bkg]}}$, and we impose loose mode-dependent requirements on the likelihood ratio $\mathcal{R}_{s/b} \equiv \mathcal{L}_{\text{sig}}/(\mathcal{L}_{\text{sig}} + \mathcal{L}_{\text{bkg}})$. Figures 1.(a)-(l) show the reconstructed variables M_{bc} , ΔE and $\mathcal{R}_{s/b}$ after flavor tagging and vertex reconstruction (before vertex reconstruction for the decay $B^0 \rightarrow K_S^0\pi^0$); the corresponding signal yields are summarized in Table I.

TABLE I: Estimated signal yields N_{sig} in the signal region for each mode.

Mode	ξ_f	N_{sig}
ωK_S^0	-1	118 ± 18
$f_0 K_S^0$	+1	377 ± 25
$K_S^0\pi^0$	-1	515 ± 32
$K^+K^-K_S^0$	$+0.86 \pm 0.18 \pm 0.09$	840 ± 34

We determine \mathcal{S}_f and \mathcal{A}_f for each mode by performing an unbinned maximum-likelihood fit to the observed Δt distribution. The decay rate is given by

$$\mathcal{P}(\Delta t) = \frac{e^{-|\Delta t|/\tau_{B^0}}}{4\tau_{B^0}} \left\{ 1 + q \cdot [\mathcal{S}_f \sin(\Delta m_d \Delta t) + \mathcal{A}_f \cos(\Delta m_d \Delta t)] \right\} \quad (2)$$

where τ_{B^0} is the B^0 lifetime and the b -flavor charge $q = +1(-1)$ when the tagging B meson is a B^0 (\bar{B}^0). The b -flavor of the accompanying B meson is identified by a tagging algorithm [13] that categorizes charged leptons, kaons and Λ 's found in the event. The algorithm returns two parameters: the b -flavor charge q and r , which indicates the tag quality as determined from MC simulation and varies from $r = 0$ for no flavor discrimination to $r = 1$ for unambiguous flavor assignment. If $r \leq 0.1$, we set the wrong tag fraction to 0.5, and therefore the accompanying B meson provides no tagging information in this case. Events with $r > 0.1$ are sorted into six intervals.

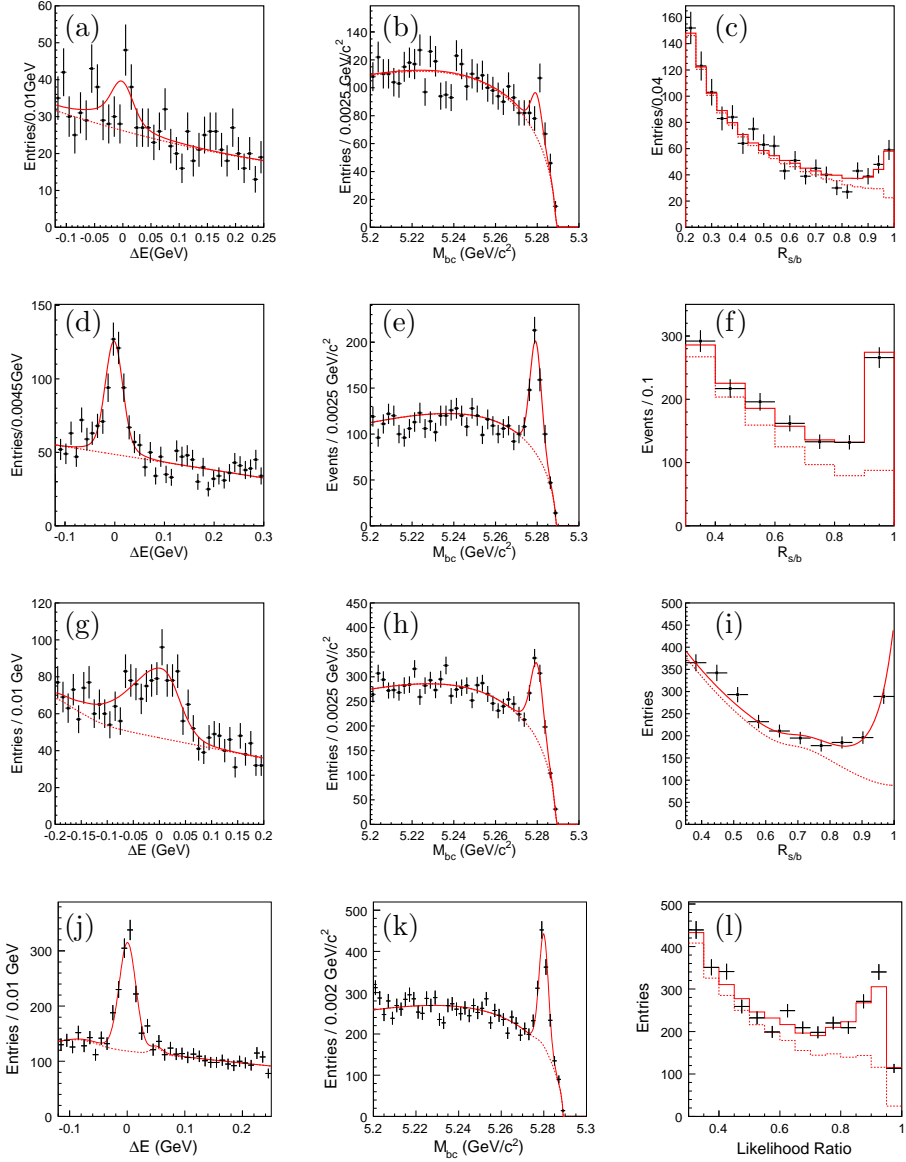


FIG. 1: ΔE , M_{bc} and $\mathcal{R}_{s/b}$ distributions for (a, b, c) $B^0 \rightarrow \omega K_S^0$, (d, e, f) $B^0 \rightarrow f_0 K_S^0$, (g, h, i) $B^0 \rightarrow K_S^0 \pi^0$ and (j, k, l) $B^0 \rightarrow K^+ K^- K_S^0$. The solid curves show the fits to signal plus background distributions, and the dashed curves show the background contributions. To enhance the signal in the ΔE and M_{bc} projections, an additional cut on $\mathcal{R}_{s/b}$ was applied (> 0.5).

To the PDF expected for the signal distribution (Eq. 2), the effect of incorrect flavor assignment is incorporated and then convolved with a resolution function $R_{\text{sig}}(\Delta t)$ to take into account the finite vertex resolution. The wrong tag fractions for the six r intervals, w_l ($l = 1, 6$), and differences between B^0 and \bar{B}^0 decays, Δw_l , as well as the resolution parameters are determined using a high-statistics control sample of semileptonic and hadronic $b \rightarrow c$ decays.

We determine the following likelihood for each event:

$$\begin{aligned}
P_i = & (1 - f_{\text{ol}}) \int \left[f_{\text{sig}} \mathcal{P}_{\text{sig}}(\Delta t') R_{\text{sig}}(\Delta t_i - \Delta t') \right. \\
& + (1 - f_{\text{sig}}) \mathcal{P}_{\text{bkg}}(\Delta t') R_{\text{bkg}}(\Delta t_i - \Delta t') \Big] d(\Delta t') \\
& + f_{\text{ol}} P_{\text{ol}}(\Delta t_i).
\end{aligned} \tag{3}$$

The signal probability f_{sig} depends on the r region and is calculated on an event-by-event basis as a function of M_{bc} , ΔE and $\mathcal{R}_{\text{s/b}}$ (and $M(\pi^+ \pi^- \pi^0)$ for $B^0 \rightarrow \omega K_S^0$). For $B^0 \rightarrow f_0(980) K_S^0$, this fit yields the number of $B^0 \rightarrow \pi^+ \pi^- K_S^0$ candidates that have $\pi^+ \pi^-$ invariant mass within the $f_0(980)$ resonance region, which includes other contributions (e.g. $B^0 \rightarrow \rho^0 K_S^0$, $K^* \pi^\pm$ and non-resonant three-body decays) which peak like the signal in ΔE and M_{bc} distributions. To estimate these peaking backgrounds, we perform a fit to the $\pi^+ \pi^-$ invariant mass distribution for the events inside the ΔE - M_{bc} signal region (Fig 2).

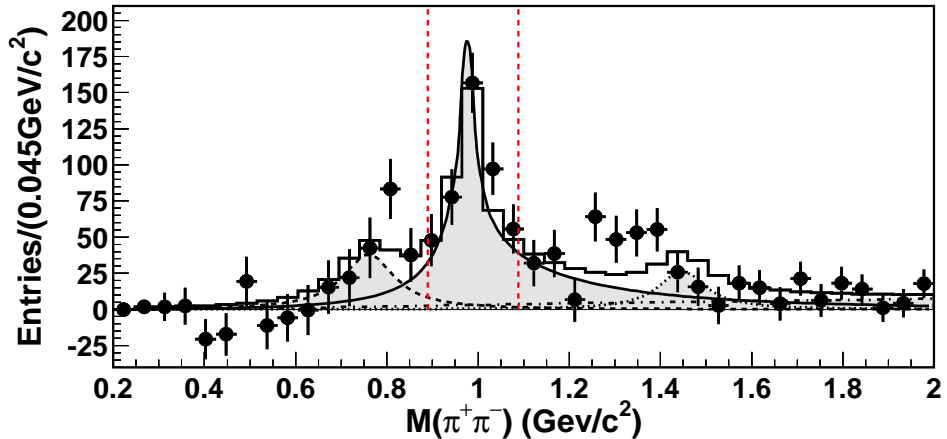


FIG. 2: $\pi^+ \pi^-$ mass distribution for the $f_0 K_S$ events in the ΔE - M_{bc} signal box (shown here after background subtraction). The histogram is the result of the fit whereas the different contributions are shown (continuous line for $f_0(980)$, dashed for ρ^0 and dotted for f_X).

The PDF for background events, $\mathcal{P}_{\text{bkg}}(\Delta t)$, is modeled as a sum of exponential and prompt components and is convolved with a sum of two Gaussians, R_{bkg} . Parameters in $\mathcal{P}_{\text{bkg}}(\Delta t)$ and R_{bkg} for background are determined from a fit to the Δt distribution for events in the ΔE - M_{bc} data sideband. $P_{\text{ol}}(\Delta t)$ is a broad Gaussian function that represents an outlier component with a small fraction f_{ol} . The only free parameters in the final fits are \mathcal{S}_f and \mathcal{A}_f , which are determined by maximizing the likelihood function $L = \prod_i P_i(\Delta t_i; \mathcal{S}_f, \mathcal{A}_f)$ where the product is over all events.

Table II summarizes the fit results of $\sin 2\phi_1^{\text{eff}}$ and \mathcal{A}_f . For the $B^0 \rightarrow K^+ K^- K_S^0$ decay, the SM prediction is given by $\mathcal{S}_f = -(2f_+ - 1) \sin 2\phi_1^{\text{eff}}$. The effective $\sin 2\phi_1$ value for this mode is found to be $+0.68 \pm 0.15 \pm 0.03^{+0.21}_{-0.13}$. The third error is an additional systematic error arising from the uncertainty of the $\xi_f = +1$ fraction. We define the raw asymmetry in each Δt bin by $(N_{q=+1} - N_{q=-1}) / (N_{q=+1} + N_{q=-1})$, where $N_{q=+1(-1)}$ is the number of observed candidates with $q = +1(-1)$. Figure 3 shows this asymmetry for good tag quality ($r > 0.5$) events in each mode. The dominant sources of systematic error for \mathcal{S}_f in $b \rightarrow s\bar{q}q$ modes are the uncertainties in the vertex reconstruction (0.01), in the background fraction (from 0.01 for $K_S \pi^0$ to 0.04 in ωK_S^0) and in the background Δt distribution (0.04 in $K_S \pi^0$

TABLE II: Results of the fits to the Δt distributions. The first error is statistical and the second error is systematic. The third error for $\sin 2\phi_1^{\text{eff}}$ of $K^+K^-K_S^0$ is an additional systematic error arising from the uncertainty of the $\xi_f = +1$ fraction.

Mode	$\sin 2\phi_1^{\text{eff}}$	\mathcal{A}_f
ωK_S^0	$+0.11 \pm 0.46 \pm 0.07$	$-0.09 \pm 0.29 \pm 0.06$
$f_0 K_S^0$	$+0.18 \pm 0.23 \pm 0.11$	$-0.15 \pm 0.15 \pm 0.07$
$K_S^0 \pi^0$	$+0.33 \pm 0.35 \pm 0.08$	$-0.05 \pm 0.14 \pm 0.05$
$K^+K^-K_S^0$	$+0.68 \pm 0.15 \pm 0.03^{+0.21}_{-0.13}$	$-0.09 \pm 0.10 \pm 0.05$

and 0.01 or less in others), and in the resolution function (0.05 for ωK_S and $K_S \pi^0$). The dominant sources for \mathcal{A}_f are the effects of tag-side interference [14] (0.04), the uncertainties in the vertex reconstruction (0.02), in the background fraction (0.03 for $f_0 K_S^0$ and ωK_S^0 and < 0.02 for others). For the $f_0 K_S^0$ mode, additional systematics were included: uncertainties from the $M(\pi\pi)$ fit (0.06 for \mathcal{S}_f) and from the assumption on the CP content of the peaking background (0.08 for \mathcal{S}_f and 0.04 for \mathcal{A}_f). For the $K_S^0 \pi^0$ mode, the uncertainty on the rare B component is taken into account (0.04 for \mathcal{S}_f and 0.02 for \mathcal{A}_f). Other contributions come from uncertainties in wrong tag fractions, lifetime and mixing. A possible fit bias is examined by fitting a large number of MC events. We add each contribution in quadrature to obtain the total systematic uncertainty.

In summary, we have performed improved measurements of CP -violation parameters $\sin 2\phi_1^{\text{eff}}$ and \mathcal{A}_f for $B^0 \rightarrow \omega K_S^0$, $f_0(980)K_S^0$, $K_S^0 \pi^0$ and $K^+K^-K_S^0$ using $535 \times 10^6 B\bar{B}$ events. Comparing the results for each individual $b \rightarrow s$ mode with those from the $B^0 \rightarrow J/\psi K^0$ decay, we have not observed a significant deviation with the present statistics.

Acknowledgments

We thank the KEKB group for the excellent operation of the accelerator, the KEK cryogenics group for the efficient operation of the solenoid, and the KEK computer group and the National Institute of Informatics for valuable computing and Super-SINET network support. We acknowledge support from the Ministry of Education, Culture, Sports, Science, and Technology of Japan and the Japan Society for the Promotion of Science; the Australian Research Council and the Australian Department of Education, Science and Training; the National Science Foundation of China and the Knowledge Innovation Program of the Chinese Academy of Sciences under contract No. 10575109 and IHEP-U-503; the Department of Science and Technology of India; the BK21 program of the Ministry of Education of Korea, the CHEP SRC program and Basic Research program (grant No. R01-2005-000-10089-0) of the Korea Science and Engineering Foundation, and the Pure Basic Research Group program of the Korea Research Foundation; the Polish State Committee for Scientific Research; the Ministry of Science and Technology of the Russian Federation; the Slovenian Research Agency; the Swiss National Science Foundation; the National Science Council and the Ministry of Education of Taiwan; and the U.S. Department of Energy.

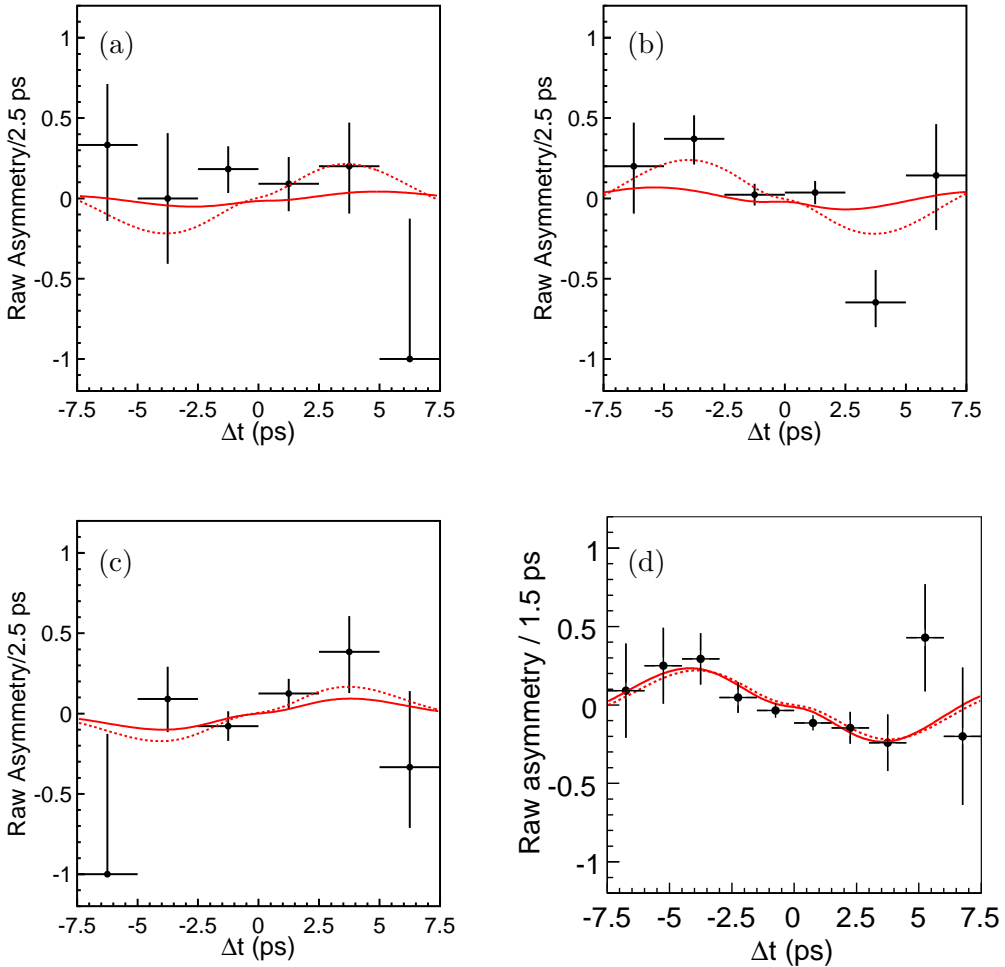


FIG. 3: Asymmetries of good-tagged events ($r > 0.5$) for (a) $B^0 \rightarrow \omega K_S^0$, (b) $B^0 \rightarrow f_0(980)K_S^0$, (c) $B^0 \rightarrow K_S^0\pi^0$ and (d) $B^0 \rightarrow K^+K^-K_S^0$. The solid curves show the results of the unbinned maximum-likelihood fits. The dashed curves show the SM expectation with the measurement of CP -violation parameters for the $B^0 \rightarrow J/\psi K^0$ mode ($\sin 2\phi_1 = +0.642$ and $\mathcal{A}_f = 0$)

-
- [1] M. Kobayashi and T. Maskawa, Prog. Theor. Phys. **49**, 652 (1973).
 [2] Y. Grossman and M. P. Worah, Phys. Lett. B **395**, 241 (1997); R. Fleischer, Int. J. Mod. Phys. A **A**, 2459 (1997); M. Ciuchini, E. Franco, G. Martinelli, A. Masiero and L. Silvestrini, Phys. Rev. Lett. **79**, 978 (1997); D. London and A. Soni, Phys. Lett. B **407**, 61 (1997).
 [3] Heavy Flavour Averaging Group, E. Barberio *et al.*, hep-ex/0603003. See <http://www.slac.stanford.edu/xorg/hfag/> for updated results.
 [4] M. Gronau and J.L. Rosner, Phys. Rev. D **59**, 113002 (1999).
 [5] D. Atwood and A. Soni, Phys. Rev. D **58**, 036005 (1998); M. Gronau, Phys. Lett. B **627**, 82 (2005).

- [6] A. Garmash *et al.* (Belle Collaboration), Phys. Rev. D **69**, 012001 (2004).
- [7] K-F. Chen *et al.* (Belle Collaboration), Phys. Rev. D **72**, 012004 (2005).
- [8] B. Aubert *et al.* (BaBar Collaboration) Phys. Rev. D **71**, 111102 (2005).
- [9] S. Eidelman *et al.* (Particle Data Group), Phys. Lett. B **592**, 1 (2004).
- [10] A. Abashian *et al.* (Belle Collaboration), Nucl. Instr. and Meth. A **479**, 117 (2002).
- [11] Y. Ushiroda (Belle SVD2 Group), Nucl. Instr. and Meth.A **511**, 6 (2003).
- [12] The Fox-Wolfram moments were introduced in G. C. Fox and S. Wolfram, Phys. Rev. Lett. **41**, 1581 (1978). The Fisher discriminant used by Belle, based on modified Fox-Wolfram moments (SFW), is described in K. Abe *et al.* (Belle Collaboration), Phys. Rev. Lett. **87**, 101801 (2001) and K. Abe *et al.* (Belle Collaboration), Phys. Lett. B **511**, 151 (2001).
- [13] H. Kakuno *et al.* (Belle Collaboration), Nucl. Instr. and Meth.A **533**, 516 (2004).
- [14] O. Long, M. Baak, R. N. Cahn and D. Kirkby, Phys. Rev. D **68**, 034010 (2003).